Adaptive Pulse Repetition Frequency Technique for an Ultrasonic Transit-Time Gas Flowmeter for Hot Pulsating Gases

Mario Kupnik, Andreas Schröder, Paul O'Leary, *Member, IEEE*, Ewald Benes, *Member, IEEE*, and Martin Gröschl

***Abstract*—A technique of using an adaptive pulse repetition frequency (PRF) to operate an ultrasonic contrapropagation transit-time gas flowmeter (UFM) is introduced. This adaptive PRF technique allows transient measurements of hot (up to 450 °C) and pulsating (up to 1.5 kHz) gas flows. Such conditions occur in the exhaust gas of a combustion engine. Here, a UFM with the widely used fixed PRF technique is not applicable, because the large gas temperature variations would prevent a reliable detection of ultrasonic pulse arrival times. Coherently reflected waves are generated within the gas because of the unavoidable acoustic impedance mismatch between the gas and the transducers, and, depending on the gas temperatures, these echoes overlap with the main signal. The adaptive PRF technique overcomes this problem and allows correct pulse detection over the whole temperature range required. The UFM utilizes special high-temperature-resistant capacitance ultrasonic transducers (CUTs) to meet the requirements in terms of operating temperature range and dynamic response. Results, which are obtained with a preliminary laboratory prototype, are presented for the exhaust gas mass flow rate in a ∅ 50-mm pipe measured at gas temperatures of up to 450 °C and at PRFs of up to 5.5 kHz, which is an increase in frequency response of one order of magnitude in comparison to existing measurement systems.**

***Index Terms*—Adaptive pulse repetition frequency (PRF), capacitance ultrasonic transducer (CUT), exhaust gas, high temperature, mass flow sensor, pulsating gas flow, ultrasonic flowmeter.**

I. Introduction

TODAY, several authorities, such as the European Commission and the Environmental Protection Agency (EPA, California), are the driving forces behind legal requirements concerning automobile exhaust emission regulations [1].

Because of the decreasing exhaust emission limits, today's requirements for the measurement of exhaust gas mass flow are demanding. Calculation of the mass flow of each exhaust emission component in kilograms per hour or grams per kilometer requires measurement of the mass flow value moment by moment. That is to say not only the accurate measurement of the averaged exhaust gas mass flow over a specific time period is required, but the transient measurement of the exhaust gas mass flow is as well. In combination with fast gas analyzer benches, this would enable the determination of the mass emission of all gas components with time resolutions below 1 ms. This additional information extracted from the exhaust gas train could facilitate the optimization and monitoring of the combustion process, the catalytic converter, and the exhaust gas train. Therefore, it may be concluded that, because of the stringent exhaust emission limits, all combustion engine manufacturers are highly motivated to obtain such a measurement system.

In the last ten years, the measurement principle of the ultrasonic contrapropagation transit-time gas flowmeter (UFM) has been applied to direct flow measurement within raw exhaust gas of automotive combustion engines. In this context, three different basic approaches concerning the realization of the flowmeter, more specifically, concerning the ultrasonic transducers utilized in the flowmeter, can be distinguished.

1) In 1998, a UFM utilizing high-temperature-resistant piezoelectric composite transducers was reported [2]. The composite transducers consisted of arrays of piezoelectrically active rods aligned in parallel, which were imbedded in a three-dimensional polymer matrix. The lead zirconate titanate (PZT) material PZ 29 (Ferropern, Kvistgård, Denmark) with a specified Curie temperature of 300 °C was used for the rods. The transducers were water-cooled with the goal of increasing the temperature range of the flowmeter up to 600 °C. In [2], only measurement results for engine rotation speeds of up to 1500 r/min were presented. The reason for this seems to be the low attainable pulse repetition frequency (PRF) of the realized flowmeter ($\approx$ 400 Hz), which is due to the fact that the piezoelectric composite transducers used had a pronounced resonant frequency with small bandwidth, e.g., [3]–[5].
2) Also in the year 1998, another concept was proposed in [6]. A transducer based on an electrical spark discharge utilizing a high-voltage source was employed to generate a pressure pulse accompanied by light emission and electromagnetic energy. A detailed description of

Manuscript received June 1, 2005; accepted July 14, 2005. This work was supported in part by AVL List GmbH, Graz, Austria. The work of M. Kupnik was supported by the FWF Austrian Science Fund. The associate editor coordinating the review of this paper and approving it for publication was Prof. Fahrettin Degertekin.

M. Kupnik is with the Edward L. Ginzton Laboratory, Stanford University, Stanford, CA 94305-4088 USA (e-mail: kupnik@stanford.edu).

A. Schröder was with the Institute of General Physics, Vienna University of Technology, 1040 Vienna, Austria. He is now with the Acoustic Monitoring Group, Preparatory Commission for the Comprehensive Nuclear-Test-Ban Treaty Organization, 1400 Vienna, Austria (e-mail: schroeder@iap.tuwien.ac.at).

P. O'Leary is with the Institute for Automation, University of Leoben, A-8700 Leoben, Austria (e-mail: oleary@unileoben.ac.at).

E. Benes and M. Gröschl are with the Institute of General Physics, Vienna University of Technology, 1040 Vienna, Austria (e-mail: benes@iap.tuwien.ac.at; groeschl@iap.tuwien.ac.at).

Digital Object Identifier 10.1109/JSEN.2006.876042

this flowmeter, which includes the transmitting transducer (spark transducer), can be found in the patents filed to the company Peus-Systems, Bruchsal, Germany [7], [8]. Two spark transducers were located in sockets attached to the wall of the measuring pipe. The generated ultrasonic pulses were deflected by deflection mirrors toward the respective directions of the crossed sound paths through the pipe. The main drawback of this concept is that the spark transducer does not provide a reciprocal effect for receiving ultrasound, such as what piezoelectric or capacitance ultrasonic transducers (CUTs) do. Therefore, again, piezoelectric transducers, which are located in the surfaces of the deflection mirrors, had to be used for receiving the ultrasonic pulses. The pulses had to pass long start-up lengths before propagating through the gas flow in the measuring pipe. Another drawback was the complexity of the construction of the transmitting transducers. Due to the fact that the electrodes successively burn down, they must be readjusted continuously. The maximum attainable PRF of this system was specified as 500 Hz [6]. Further, the range of the mean temperature was specified as -50 °C to 800 °C, but no measurement results at temperatures higher than 250 °C were presented. Up to now, this measurement system is not available commercially for exhaust gas, but in 2001, the same system was announced [9] as a flowmeter for air intake measurements with PRFs of up to 500 Hz.

3) To the authors' knowledge, up to now, the company Sick Maihak, Reute, Germany, is the only supplier that offers a commercial UFM (FLOWSIC 150 Carflow), which is designed for measuring the volumetric flow rate on automotive roll test stands and road test simulators directly in the raw exhaust gas [10]. However, due to the fact that piezoelectric transducers are used in this flowmeter, the maximum allowable temperatures are limited. The maximum transducer temperature is 220 °C, and the maximum allowable gas temperature is 250 °C ($<$ 10 min/h). In addition, the maximum PRF is specified as 75 Hz [10]. Therefore, it may be concluded that, due to the use of piezoelectric transducers, this flowmeter is limited with respect to its applicability in the raw exhaust gas of automotive combustion engines.

In our approach for measuring the exhaust gas mass flow directly in the exhaust gas train of an automotive combustion engine, we also apply the measurement principle of the UFM. A high-temperature-resistant broadband CUT is used both for transmitting and receiving the ultrasonic pulses [11]. Nowadays, CUTs are accepted as state-of-the-art transducers for gas flow measurement applications, e.g., [12]. By modifying the construction of the commonly used CUTs, which, for instance, utilize a metallized polymer membrane as the moving electrode, and by selecting appropriate transducer materials, we have achieved a wideband CUT for operation at elevated gas temperatures of up to several hundred degrees Celsius. This transducer also features better overall acoustic characteristics in comparison to the state-of-the-art transducer, e.g., [13]–[15]. In addition to the extended operating temperature range, the main advantage of this type of transducer is its wide signal bandwidth, which allows to operate the UFM at high PRFs. Furthermore, this transducer shows excellent coupling characteristics to gaseous media. The transducer makes use of a patterned thermally oxidized silicon backplate, which is covered by a titanium foil as the moving membrane. Details concerning the structure, the fabrication steps, and the specifications of this CUT can be found in [11] and [16].

At this stage, it should be emphasized that this type of CUT has the potential of filling the significant gap concerning a transducer technology enabling air-coupled ultrasonic wave generation and reception both in hot gaseous media and at high PRFs. Particular state-of-the-art transducer technologies allow air-coupled ultrasonic wave generation and reception at elevated gas temperatures but only with a low PRF, e.g., [3]–[5]. Other transducer technologies provide excellent broadband characteristics, i.e., high PRFs, but suffer from their low operating temperature range, e.g., [17]. Buffered transducers, e.g., [18], can operate at gas temperatures of up to 600 °C but appear limited at present to PRFs in the range from 100 to about 1000 Hz, and because of their rigid metallic construction, they are not as well matched to the low acoustic impedance of hot gas as the CUT. Only a broadband high-temperature-resistant CUT enables a PRF in the range of several kilohertz, which is essential for transient gas flow metering in a hot and pulsating exhaust gas flow.

With the use of this high-temperature-resistant capacitance transducer, the well-known UFM principle, e.g., [19], is applicable for the first time in the demanding environment of an automotive exhaust gas train over a wide temperature range (up to 450 °C). This paper, which is an extended version of our conference paper presented at IEEE Sensors 2004 [20], is focused on a technique for adjusting the PRF, depending on the temperature of the gas. This adaptive PRF technique is essential for the successful application of a UFM directly in the exhaust gas train of an automotive combustion engine. An example for another field of application, where an adaptive PRF technique has been used to improve the probability of correct signal detection, are air-to-air radar systems, e.g., [21].

When applied to the UFM measurement principle, the adaptive PRF technique overcomes the fundamental problems associated with the range and dynamics of the exhaust gas temperature and the gas flow pulsations.

II. Experimental Setup

The measurement configuration as used in this work consists of a centric double-path UFM with a circular measuring pipe ($R = 25$ mm) and with a sound path inclination angle $\alpha = 30°$, as depicted in Fig. 1(a). Two pairs of diametrically opposed transducers were mounted in a so-called wetted configuration (i.e., in direct contact to the gas) [19], with the transducer membranes close to the pipe wall. Thereby, protrusion of the transducers into the main flow was avoided to ensure a low pressure drop caused by the flowmeter, and the size of the remaining transducer port cavities was minimized. An enlarged view of one transducer port cavity is depicted in Fig. 1(b).

The UFM was operated in burst mode, i.e., three-cycle sinusoidal tone burst signals in the frequency range from 350

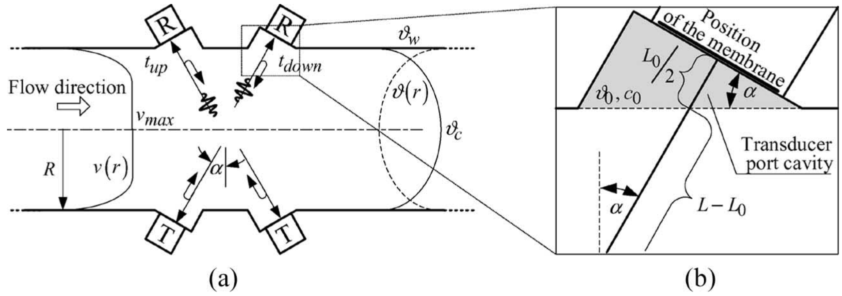

Fig. 1. (a) Schematic of a centric circular-pipe double-path ultrasonic flowmeter. The gas flow velocity and temperature distributions ($v(r)$ and $\vartheta(r)$), reflections at the receiver (R) and transmitter (T) positions, pulse propagation times ($t_{\rm up}$ and $t_{\rm down}$), and wall and core temperatures ($\vartheta_{\rm w}$ and $\vartheta_{\rm c}$) are indicated. (b) Enlarged view of one transducer port cavity, where ϑ_0 and c_0 are the temperature and the speed of sound, respectively, inside the transducer port cavity, L is the distance between the membranes, and L_0 is the mean total depth of the two cavities in each sound path.

to 500 kHz [22] were supplied to the transmitting transducers (T). A minimum of three cycles was chosen to guarantee that the maximum signal amplitude was reached during each burst.

The velocity v (mean value along the two sound paths) of the gas flow and the temperature-dependent speed of sound c (mean value along the two sound paths) were calculated from the measured pulse propagation times $t_{\rm up}$ and $t_{\rm down}$ in the upstream and downstream directions, respectively. The double-path configuration was chosen to enable the simultaneous measurement of $t_{\rm up}$ and $t_{\rm down}$. Simultaneous measurement is essential for fast UFM response and precise measurements in pulsating gas flows. It is important to notice that for the configuration according to Fig. 1, the following set of appropriate equations is required for the calculation of v and c:

$$v = \frac{1}{2\sin(\alpha)} \frac{(t_{\rm up} - t_{\rm down})(L - L_0)c_0^2}{(L_0 - c_0 t_{\rm up})(L_0 - c_0 t_{\rm down})} \quad (1)$$

$$c = -\frac{1}{2} \frac{(2L_0 - c_0 t_{\rm up} - c_0 t_{\rm down})(L - L_0)c_0}{(L_0 - c_0 t_{\rm up})(L_0 - c_0 t_{\rm down})} \quad (2)$$

where L is the distance between the membranes, and c_0 is the mean speed of sound inside the transducer port cavities. These equations take into account the additional pulse propagation times L_0/c_0 caused by the transducer port cavities with the mean total depth L_0 [Fig. 1(b)] in each sound path. Two assumptions were made for the derivation of these equations, namely 1) there are no temperature gradients inside the transducer port cavities, and 2) the ultrasonic pulses are affected by the gas flow only on the sound path located inside the measurement pipe, i.e., on the distance $L - L_0$, as indicated in Fig. 1(b). A local temperature measurement inside the transducer port cavity (ϑ_0) enables the calculation of the speed of sound c_0 from

$$c_0 = \sqrt{\frac{\kappa(\vartheta_0) R_{\rm gas}(\vartheta_0 + 273.15)}{M}} \quad (3)$$

where $\kappa = c_P/c_V$ is the temperature-dependent adiabatic coefficient, i.e., the ratio of the specific heat capacity at constant pressure c_P to the specific heat capacity at constant volume c_V, $R_{\rm gas}$ is the universal molar gas constant (8.31441), and M is the molecular weight of the gas. Using an appropriate meter factor k_v allows one to calculate the velocity v_A, i.e., the gas flow velocity averaged over the cross-sectional area A of the measuring pipe directly from v [19]. Therefore, the mass flow rate Q_m (in kilograms per hour) can be written as [23]

$$Q_m = 3600 v k_v A \frac{P\kappa(\vartheta)}{c^2} \quad (4)$$

where ϑ is the temperature averaged over the travel paths of the ultrasonic pulses, and P is the absolute pressure measured inside the pipe, which ideally corresponds to the pressure at the intersection point of the two sound beams.

In general, the exhaust gas flow of an automotive combustion engine is characterized by large temperature variations and by strong and fast mass flow pulsations. Due to the thermal inertia of the measuring pipe, steep temperature gradients between the wall and the center of the pipe may occur, depending on the changes of engine load conditions during operation. Positive or negative temperature gradients along the sound paths, as indicated in Fig. 1(a), lead to disturbing refraction effects superimposed on the desired beam deflection (“sound drift”) caused by the velocity of the gas flow [24]. Therefore, during UFM operation, the wall temperature of the measuring pipe was kept at about 150 °C by means of electrical heating elements to reduce temperature gradients and associated disturbing effects.

The requirements concerning the PRF of a UFM utilized for mass flow measurements in an exhaust gas train of a typical automotive combustion engine were analyzed in [23]. The minimum PRF for end-of-pipe measurements to allow transient detection of the pulsating gas flow was established as about 500 Hz, whereas for measurements closely upstream of the catalytic converter, the required PRF was found to be about 5 kHz. A commonly used range of operation of the combustion engine was the underlying assumption for these limits.

III. Problem Analysis and Method

A. Thermally Induced Overlapping of Ultrasonic Pulses

Because of the wide temperature range and the high PRFs required, pulse overlapping effects inevitably prevent a correct pulse arrival time detection over the whole gas temperature range, if a constant PRF is used. This can be explained as follows.

When both transmitters (T) are triggered to emit an ultrasonic pulse, two ultrasonic waves propagate through the gas in the flowmeter. After the travel times $t_{\rm up}$ and $t_{\rm down}$, respectively,

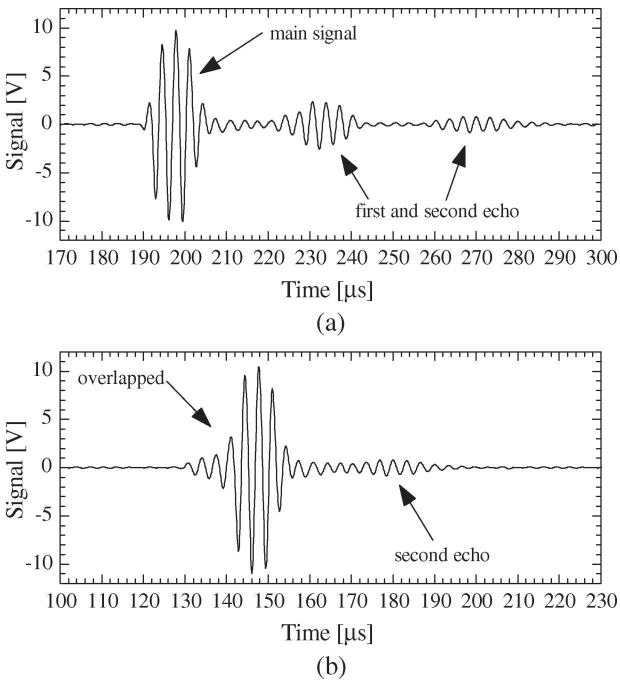

Fig. 2. (a) Receiver signal separated from the first and second echoes. (b) Receiver signal overlapped with the first echo. (Only one channel is shown.)

which are dependent on the gas velocity v, on the length of the travel path L, and on the temperature-dependent speed of sound c [25], the ultrasonic wavefronts arriving at the receiving transducers (R) cause displacements of the membranes, and therefore, electrical signals are generated. These main signals in both channels, i.e., upstream and downstream, indicate the exact travel times of the ultrasonic pulses propagating from the respective transmitter to the opposed receiver. At room temperature, the main signal [Fig. 2(a), only one channel is shown for clarity] occurs at approximately 190 μs after the time of triggering the transmitter. In this example, a sinusoidal tone burst signal with a signal frequency $f = 350$ kHz, and a duration of three cycles was applied to the transmitting transducers.

Because the acoustic impedances of the gas and the transducers are unavoidably mismatched, the ultrasonic pulses propagating in the gas are partially reflected with a phase shift of 180° each time a gas–membrane interface is reached. The first such reflections occur at the receiving transducers. The reflected parts of the ultrasonic waves [see arrows in Fig. 1(a)] travel back to the transmitters, where, again, reflections with a phase shift of approximately 180° occur. Due to the two consecutive phase shifts of 180° in each sound path, coherently reflected waves are generated, which travel in substantially the same directions as the originally emitted waves, that is, from the transmitters to the receivers. While the reflected waves have essentially no influence on transmitter operation, the coherently reflected waves that arrive at the receiver positions within specific time intervals after the original signals cause additional electrical signals (echoes) at the receivers [Fig. 2(a)]. In this example, the first echo occurs at approximately 20 μs after the main signal, and it belongs to the transmitter pulse triggered one time period before the pulse that caused the main signal shown here. (PRF was $f_{\mathrm{rep}} = 3$ kHz, which corresponds to a transmitter pulse repetition time of about 333 μs.) The only difference between the main signal and the echo is the lower amplitude of the echo because of the increased overall attenuation [26], [27] along the three-times-longer travel path through the gas of this ultrasonic pulse and the additional attenuation loss at each reflection. Neglecting sound deflection effects, the flow velocity v of the gas has no significant influence on the additional propagation time, i.e., the propagation time after the first reflection of this doubly reflected pulse. This is because of the fact that the pulse then propagates in succession in both directions, i.e., upstream and downstream or vice versa.

This coherently reflected pulse is again partially reflected at the receiving transducer and subsequently at the opposed transmitter; therefore, further coherent waves and corresponding echo signals at the receivers are generated. The second echo [Fig. 2(a)] belongs to the transmitter pulse triggered one time period before the pulse that caused the first echo. The corresponding acoustic wave had experienced a five-times-longer travel path through the gas than the main pulse and four reflections in total. Therefore, the amplitude of the second echo is low compared with that of the main signal. Further echoes, i.e., third, fourth, and so on, do not have a significant influence on the receiver signal because of their low amplitudes. Thus, only the first and second echoes need to be considered for the determination of an optimum PRF (see Section III-B).

In an optimum situation concerning gas temperature and PRF, the first and second echoes occur after the main signal [Fig. 2(a)], i.e., there is no overlapping between the main signal and the echoes.

However, if the temperature of the gas is increased, the sound speed also increases [25]. Because of the higher propagation speed of the ultrasonic waves, the main signal occurs earlier [in the example shown in Fig. 2(b), it was at approximately 140 μs after the transmitter trigger pulse]. Because the travel path of the first echo pulse is three times longer and five times longer for the second echo pulse, the increasing temperature has even more influence on the total propagation time of these pulses. Therefore, the first or second echo may approach the main signal (originating from a previously triggered pulse), causing an overlapping effect [Fig. 2(b)]. In such a case, because of the coherent property of the reflected waves, it is not possible to distinguish the main signal from the echo. The exact ultrasonic pulse arrival time information is destroyed by this overlapping effect, which unavoidably may occur at certain UFM operating conditions as a consequence of the wide temperature range and high PRF required.

B. Method of Using an Adaptive PRF

The problem of overlapping receiver signals can be solved by using an adaptive PRF. The main concept is to employ the information on the gas temperature (or the actual value of the sound speed) for calculating an optimum PRF for the current UFM operating conditions and to automatically adjust the actual PRF accordingly. The optimum PRF is achieved when the first and second echoes occur clearly separated from the main signal, each after some safety time period. The schematic

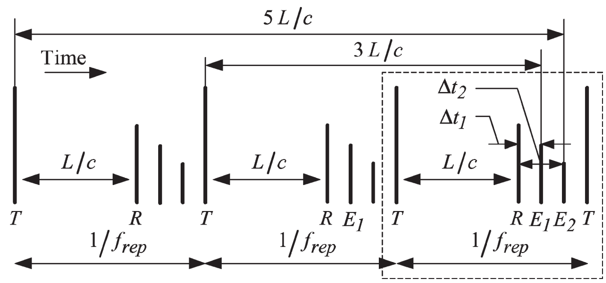

Fig. 3. Schematic of the time positions of the main signals and the echoes. L is the distance between the transmitter and the receiver, $f_{\rm rep}$ is the PRF, c is the speed of sound, R is the receiving time of the main signal, and E_1 and E_2 are the receiving times of the first and second echoes, respectively. Δt_1 and Δt_2 are the time intervals between R and E_1 and between R and E_2, respectively.

in Fig. 3 is helpful to derive the equations for the calculation of this optimum PRF. The signals and echoes are depicted by vertical lines. Only one channel of the flowmeter is considered here, which is sufficient because of the small time difference between the corresponding upstream and downstream signals in comparison to the ultrasonic pulse propagation times. After each time period $1/f_{\rm rep}$, the transmitting transducer is triggered to emit an ultrasonic pulse. These points in time are labeled with T. At a certain period after each transmitting point in time, the main signal R occurs at the receiver position. This travel time period, neglecting the influence of the velocity of the gas, is given by L/c, where L is the distance between the transmitter and the receiver, and c is the speed of sound. If the region within the dashed-line rectangle is considered, it is evident that the first echo E_1 is caused by the transmitter signal triggered one time period before T, and therefore, the total travel time of this reflected wave is $3L/c$. Concerning the second echo E_2, the travel time is $5L/c$. The safety time interval between the main signal R and the first echo E_1 is termed Δt_1, and for the second echo, it is Δt_2.

Concerning the safety time Δt_1, i.e., the temporal position of the first echo with respect to the main signal, the following equation must be fulfilled:

$$3\frac{L}{c} - \frac{1}{f_{\rm rep}} - \frac{L}{c} = \Delta t_1. \tag{5}$$

Concerning the safety time Δt_2, i.e., the temporal position of the second echo in relation to the main signal, the respective equation is

$$5\frac{L}{c} - 2\frac{1}{f_{\rm rep}} - \frac{L}{c} = \Delta t_2. \tag{6}$$

Dividing (6) by (5) gives $\Delta t_2/\Delta t_1 = 2$. That is, if the first echo E_1 occurs with a certain safety time interval Δt_1 after the main signal R, the second echo E_2 occurs with the same safety time $\Delta t_2 - \Delta t_1 = \Delta t_1$ after the first echo. Thus, (5) is sufficient to determine the optimum PRF $f_{\rm rep}$, i.e.,

$$f_{\rm rep} = \frac{c}{2L - c\Delta t_1}. \tag{7}$$

Equation (7) shows that the optimum PRF, termed $f_{\rm rep}$, can be calculated from the geometric parameter L, the temperature-dependent speed of sound c, and the chosen safety time interval Δt_1. It is desirable to set this safety time Δt_1 as small as possible to enable high PRFs. An optimum value for Δt_1 can be found, when the duration of the receiver signal and the influence of the gas flow velocity are additionally taken into account.

The duration of the receiver main signal can be estimated as follows: Because three cycles, i.e., three full oscillation periods, are required for full excitation of the transmitting transducer, the receiving transducer will show approximately (worst case) three significant postoscillations [see Fig. 2(a)]. Thus, with the signal frequency f, the total duration of the receiver main signal can be estimated as $6/f$ according to the three cycles of the excitation signal plus the three postoscillations.

The influence of the flow velocity of the gas must also be considered to find the optimum safety time Δt_1. In Fig. 3, this influence is neglected, i.e., a constant (not flow dependent) pulse propagation time $t = L/c$ between the transmitter and the receiver is assumed. However, when a gas flow is present, the propagation times $t_{\rm up}$ and $t_{\rm down}$ [Fig. 1(a)] are dependent on the flow velocity v and the flow direction. Thereby, the main signal and the echo pulses experience essentially the same change of propagation time with v, because the effect is compensated for the multiply reflected waves, as discussed in the previous section. In Fig. 3, this would mean that the time points R, E_1, and E_2 are shifted together toward (for the downstream measuring path) or away from the transmitter trigger point T (upstream measuring path). With a given geometry (α, L, L_0) of the flowmeter, a given maximum gas flow velocity, and the minimum value of the sound speed at the lowest gas temperature, the maximum shifts $(t_{\rm up})_{\max}$ and $(t_{\rm down})_{\max}$ can be calculated with (1) and (3). This calculation delivers a value

$$\Delta t = (t_{\rm up})_{\max} - (t_{\rm down})_{\max} \tag{8}$$

for the minimum safety time that accounts for the gas flow dynamics. This time is the minimum safety time interval required between the ending of the main signal and the beginning of the first echo. Thus, the optimum total safety time Δt_1 that accounts both for the gas flow dynamics and the receiver signal duration can be calculated as

$$\Delta t_1 = 6\frac{1}{f} + \Delta t. \tag{9}$$

Equation (9) is substituted into (7) to obtain the final equation

$$f_{\rm rep} = \frac{cf}{f(2L + c\Delta t) - 6c} \tag{10}$$

for calculating the optimum PRF. With knowledge of the temperature-dependent actual value of the sound speed c in the gas, the current PRF can be continuously adjusted to the optimum value, depending on the actual UFM operating conditions. Thereby, explicit measurement of the gas temperature for this purpose is not required, because the sound speed can be calculated directly from measured pulse propagation times with sufficient accuracy (2).

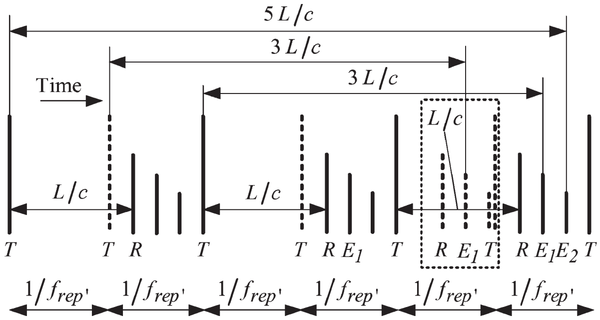

Fig. 4. Schematic of the time positions of the main signals and echoes for interlaced UFM operation mode (see Fig. 3).

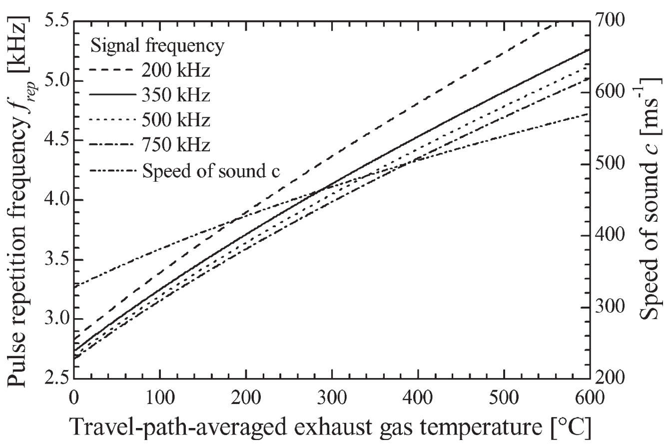

Fig. 5. Temperature-dependent optimum PRF calculated according to (10). Different signal frequencies for the transmitting transducers are compared. A sinusoidal burst signal with three full-wave trains is assumed. Further, the speed of sound c, which was calculated according to (3), is shown.

C. Interlaced Mode of UFM Operation

The underlying assumption of Fig. 3 and of the derivation of (10) is that the ultrasonic pulses (main signal) are already received before the next pulses are transmitted. However, there is no need to wait for the next trigger to transmit an ultrasonic pulse until the previous one has arrived.

If the optimum PRF f_{rep}, as calculated from (10), is simply doubled, an interlaced operation mode of the UFM with a PRF $f_{\mathrm{rep}'} = 2\ f_{\mathrm{rep}}$ is obtained (Fig. 4), which allows twice the signal sampling rate as for the normal (noninterlaced) mode. The only condition that must be fulfilled for this mode to work properly is stated as follows: The time period between the transmitting time T and the receiving time R must be large enough so that the complete time span of a receiver signal, including the main signal and the subsequent first and second echoes, fits in between. In Fig. 4, this required temporal range is indicated by the dashed-line rectangle.

IV. Results and Discussion

The variation range of the optimum PRF for the considered temperature range (0 °C–600 °C) of the gas and for the specific geometry used here (Fig. 1) is shown in Fig. 5. Further, the corresponding (temperature dependent) speed of sound values c, which are calculated with (2), are presented. With these values, the optimum PRF for the given temperature was calculated from (10), with $L = 65.24$ mm and the ultrasonic signal frequency f varying from 200 to 750 kHz. The measurement results that are shown in this section were obtained with a constant signal frequency $f = 350$ kHz (continuous line in Fig. 5) [22]. A value of 30 μs was used for the safety time interval Δt, which was calculated from (8), with $\alpha = 30°$, $L_0 = 7.5$ mm, a given maximum gas flow velocity assumed to be 50 ms^{-1} (typical value for a common automotive combustion engine), and the minimum value of the sound speed $c_{\min} = 332\ \mathrm{ms}^{-1}$ at the lowest gas temperature $\vartheta = 0$ °C. When the UFM is operated in standard (noninterlaced) mode, the optimum PRF lies between 2.5 and 5.5 kHz over the whole temperature range. In interlaced operation mode (Fig. 4), and for the same geometrical and temperature conditions as above, the optimum PRF is in the range from about 5 to 10 kHz, which is remarkable for a UFM.

The laboratory prototype of the flowmeter was used to determine the mass flow rate in an exhaust gas train of an automotive combustion engine operated in a test-bed environment. The system was installed at the end of the exhaust pipe (end-of-pipe measurement). Two different types of measurements performed are given as follows: 1) Comparative measurements at stationary engine operating points were accomplished to verify the functionality of the UFM, using the adaptive PRF technique, over a wide gas temperature range and to evaluate the measurement uncertainty of the UFM. Thereby, the reference values for the mass flow were obtained from calibrated measurement equipment available at the test bed. 2) Transient measurements were conducted at different operating points and during different changes of the operating conditions of the combustion engine to demonstrate the dynamic performance of the UFM obtained with the adaptive PRF.

The results of these experiments are presented in the following subsections, which are then followed by a brief discussion on important aspects of UFM design and operation (geometry, reduction of transducer temperature stress, and plausibility checking of results).

A. Comparative Measurement

During a measurement cycle, a total of 14 different engine operating points were set with respect to engine rotational speed and braking torque. The range of the engine speed was from 1500 to 4500 r/min, and for the braking torque, it was from 10 to 100 $\mathrm{N} \cdot \mathrm{m}$. Each operating point was kept in stationary mode for a time period of approximately 5 min to achieve stable temperature conditions in the UFM, which minimized parasitic thermally induced sound refraction effects. Then, both measurements, i.e., reference and UFM, were triggered simultaneously.

The mass flow values determined by both systems, each measured and averaged over 30 s, were compared as shown in Fig. 6(a). Fig. 6(b) depicts the relative difference between the reference values and the UFM results as a function of the mass flow. It is evident that essentially all UFM results lie within the $\pm 2\%$ uncertainty limits specified for the reference system. Further, the temperature difference between the center

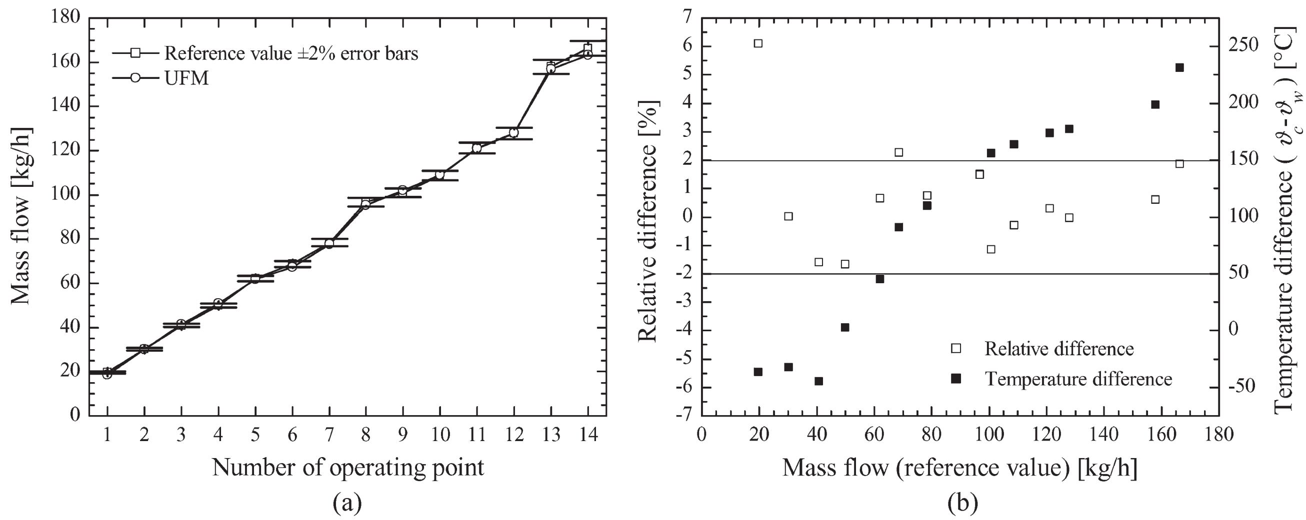

Fig. 6. Mass flow values measured with the UFM (end-of-pipe measurement) compared to reference values obtained from engine test bed equipment. (a) Absolute values. (b) Relative difference with respect to reference mass flow (horizontal lines show uncertainty limits of reference) and temperature difference between the center of the pipe (ϑ_c) and the pipe wall (ϑ_w).

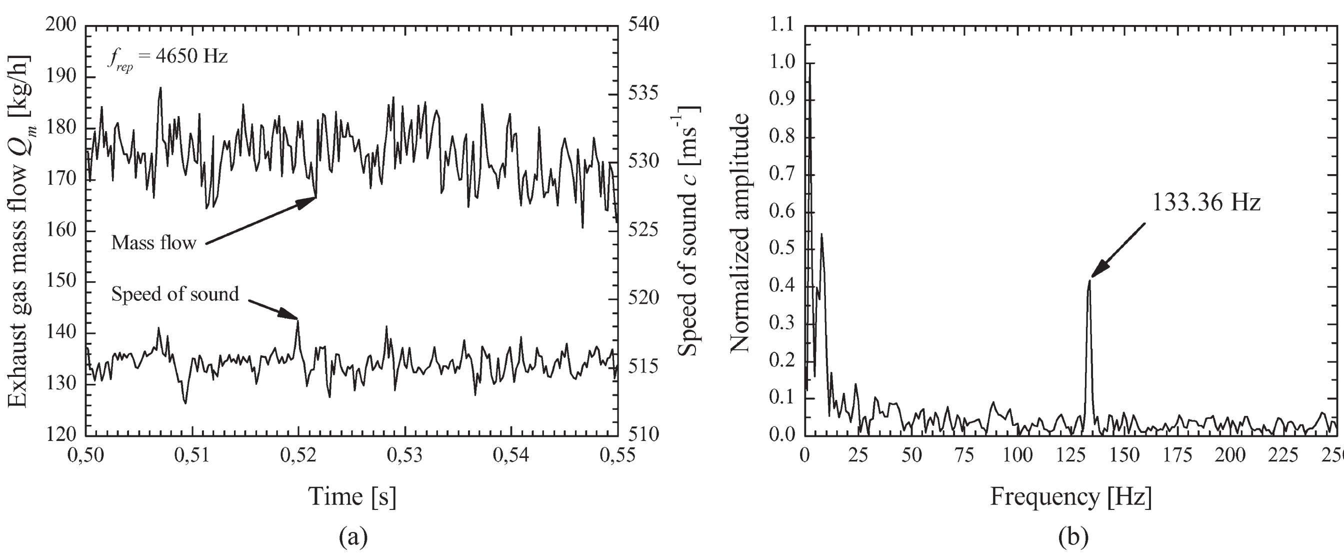

Fig. 7. Exemplary UFM measurement result for the exhaust gas mass flow of an automotive combustion engine at 4000 r/min and an exhaust gas temperature of 450 °C (end-of-pipe measurement); an optimum PRF of 4650 Hz for the given engine working conditions was used. (a) Mass flow pulsations during a time period of 50 ms. (b) Corresponding frequency spectrum.

of the pipe (ϑ_c) and the pipe wall (ϑ_w), according to the engine operating points, are shown in Fig. 6(b).

The mass flow reference values were obtained by the following method: A fuel mass flow meter (Coriolis flow meter, developed by AVL List, Graz, Austria) was employed to measure the fuel consumption of the combustion engine at each stationary operating point. With the lambda value λ, which was measured by a lambda probe, and with the known stoichiometric air requirement for the specific fuel used, the mass flow of the dry intake air was calculated. From this, the corresponding mass flow of the humid air was obtained taking into account the degree of moisture measured by a humidity sensor. The reference values for the exhaust gas mass flow were calculated as the sum of the mass flow of the humid air and the fuel consumption. This system only enables the determination of exhaust gas mass flow values averaged over time periods of $\geq$ 20 s. The specified measurement uncertainty is $\pm 2\%$, as depicted in Fig. 6. However, this value is only valid if a spark-ignition engine is used, which is operated around $\lambda = 1$, and if the mass flow averaging time is at least 30 s. Both conditions were met for the measurements presented here.

The averaged error of the mass flow measurement with the UFM was 0.66% with a standard deviation of 1.96% for mass flows in the range from 20 to 170 kg/h with gas temperatures between 20 °C and 450 °C.

B. Transient Measurement

An exemplary result of a real-time exhaust gas mass flow measurement at an engine rotational speed of 4000 r/min and an exhaust gas temperature of 450 °C (end-of-pipe measurement) is presented in Fig. 7(a). The UFM was operated with a PRF of 4650 Hz, which was the optimum value with respect to the given temperature and flow conditions inside the measuring pipe. Thus, the sampling rate for the mass flow was 4650 Hz as well. Only a small time interval of 50 ms is shown in Fig. 7(a) to make the pulsations of the mass flow visible in the diagram.

The frequency spectrum calculated from this mass flow course over a time period of 1 s is shown in Fig. 7(b). (The constant component of the mass flow was removed before calculation of the frequency spectrum.) The spectrum shows a significant peak at 133.36 Hz. This value corresponds to the rotational speed of the combustion engine. The theoretical main pulsation frequency of the exhaust gas mass flow can be calculated using

$$f_p = C_1 \frac{UZ}{60} \tag{11}$$

where C_1 is a constant ($C_1 = 1$ for two-stroke engines and $C_1 = 1/2$ for four-stroke engines), U is the engine speed in rotations per minute, and Z is the number of cylinders. Substitution of the actual value for the rotational speed $U = 4000$ r/min, and of the engine parameters ($C_1 = 1/2$ and $Z = 4$) provides the theoretical value for the exhaust gas mass flow pulsation frequency $f_p = 133.33$ Hz, which is in excellent agreement with the frequency of the peak in Fig. 7(b). The two other peaks in Fig. 7(b), which are at 2.28 and 7.98 Hz, respectively, are caused by the regulating oscillations of the synchronous machine used as load of the combustion engine at the test bed.

An interesting example for a transient change of the combustion engine's operating conditions during a mass flow measurement is a turn-off procedure, as shown in Fig. 8(a). The combustion engine was operated at a rotational speed of 2800 r/min and a braking torque of 25 N · m for about 5 min to reach a stable exhaust gas temperature of about 160 °C [Fig. 8(b)]. The last 30 s of operating the engine in this stable condition corresponds to the first 30 s on the time scales of the diagrams in Fig. 8. Then, the combustion engine was operated in idle mode (750 r/min and 10 N · m), which resulted in a drop of the exhaust gas mass flow and temperature. After 50 s of idle operation (at 80 s on the time scale), the combustion engine was turned off completely, which resulted in a return flow. This return flow (with an average value of about −1 kg/h) can be recognized in Fig. 8(a) between 80 and 100 s. It was caused by the cooling down of the exhaust gas pipe. The change of mass flow oscillations, as seen in Fig. 8(a), of around 60 s was caused by an unsuccessful attempt to turn the engine off, because the turn-off button was not pressed long enough by the operator of the test bed.

Fig. 8(b) also demonstrates the tracking of the adaptive PRF following this transient change of the UFM operating condition (gas temperature) during this turn-off procedure of the combustion engine.

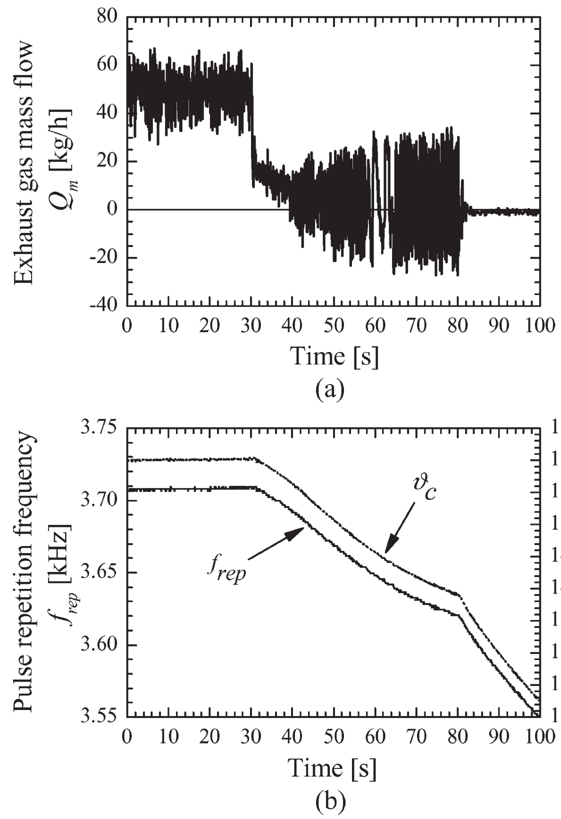

Fig. 8. Exemplary UFM measurement result for a transient temperature change of the exhaust gas during the turn-off procedure of the combustion engine. (a) Measured exhaust gas mass flow Q_m. (b) Transient change of the exhaust gas temperature ϑ_c (measured at the center of the pipe) and the optimum adaptive PRF, which was automatically tracked according to this temperature drop.

C. Discussion

In common UFM applications, an eccentric transducer arrangement is widely used, that is, where the intersection point of the sound paths has an offset from the center of the pipe. The main advantage of such a geometry is the closer distance between the receiver and the transducer, which is more significant in applications with larger pipe diameters. In this work, a centric double-path configuration (Fig. 1) was chosen, because an eccentric sound path arrangement is prevented by the thermally induced sound refraction effects that occur as a consequence of the wide gas temperature range. In an eccentric arrangement, the acoustic waves would be refracted away from the ideal sound path to the receiving transducer (toward the colder areas of the pipe), which would restrict the measurement range of the UFM. The double-path configuration, i.e., using two separate sound paths, allows the comparison of the received signal amplitudes in both channels during operation, which is advantageous, in particular, at elevated temperatures to monitor the physical conditions of the transducers.

Inside each of the transducer port cavities, there exists a flow vortex with a low gas velocity in comparison to the main gas flow. This flow vortex is partially surrounded by the wall of the measuring pipe, which, normally, is at a lower temperature than the gas. Thus, for the application discussed here, the measurement configuration as shown in Fig. 1 basically has two advantages in comparison to a configuration with the transducers showing protrusion into the main flow [12], namely 1) transducer membranes are located in regions where the temperature is lower, and 2) temperature gradients along the transducer membrane surfaces are lower due to the fact that the membranes are not located in the region (close to the center of the pipe) where the temperature distribution normally shows a steep gradient.

The effect of the transducer port cavities on measured pulse propagation times is mathematically considered (1) and (2). Therefore, the depth of the cavities could be enlarged to further reduce the thermal stress on transducers if required. Such optimization of UFM geometry is part of future work.

The travel-path-averaged speed of sound c is required for the calculation of the optimum PRF. The UFM itself provides a value for the speed of sound calculated from the two travel times (t_{up} and t_{down}). Alternatively, the measured temperature information of the gas can be used to determine c. Either an integrating temperature measurement along the pipe diameter or an appropriate temperature distribution model in combination with two or more local temperature measurements are feasible.

It is important to notice that this also enables a simple plausibility checking of the measurement values and the functionality of the transit-time detection algorithm. The value for the speed of sound calculated from the temperature information can be compared with the value for speed of sound that is directly obtained from the UFM. If the deviation exceeds a given limit, an incorrect acoustic pulse arrival time detection could be the reason, and the obtained mass flow value should be used with caution.

V. Conclusion

The adaptive PRF technique has been analyzed and proven experimentally to overcome the significant problems commonly associated with the range and dynamics of the gas temperature in a UFM operating in an exhaust gas train of an automotive combustion engine. In this application, the large temperature range inevitably prevents a correct pulse arrival time detection over the whole temperature range if a constant PRF is used, regardless of the complexity of the implemented pulse arrival time detection algorithm. The proposed technique of using a temperature-dependent adaptive PRF guarantees a correct detection of the ultrasonic pulses (bursts) over the whole temperature range. The only drawback is that for signal reconstruction, in addition to the mass flow values, time stamps must be stored. According to Shannon's sampling theorem, the presented UFM using an adaptive PRF, in interlaced or noninterlaced operation mode, enables transient measurements at all feasible measurement positions in the exhaust gas train of a common automotive combustion engine. Therefore, the UFM measurement principle can be applied efficiently in the exhaust gas train of combustion engines. This was proven by successful tests of a preliminary laboratory prototype of a UFM with adaptive PRF in a combustion engine test-bed environment.

Acknowledgment

The authors would like to thank L. Lynnworth, Lynnworth Technical Services, Waltham, MA, and Ö. Oralkan, Ginzton Laboratory, Stanford University, CA, for many fruitful discussions and for their support.

References

[1] N.-O. Nylund and A. Lawson. (2000). "Exhaust emissions from natural gas vehicles," International Association for Natural Gas, Finland, Tech. Rep. [Online]. Available: http://www.apvgn.pt/documentacao/iangv_rep_part1.pdf

[2] P. Klee and W. Gebhardt, "Die hochauflösende Messung von Abgasmassenstrom und -temperatur mittels Ultraschall," *MTZ Motortechnische Zeitschrift*, vol. 59, no. 3, pp. 188–194, 1998 (in German).

[3] I. Ladabaum, X. Jin, H. T. Soh, A. Atalar, and B. T. Khuri-Yakub, "Surface micromachined capacitive ultrasonic transducers," *IEEE Trans. Ultrason., Ferroelectr., Freq. Control*, vol. 45, no. 3, pp. 678–690, May 1998.

[4] D. A. Hutchins, D. W. Schindel, A. G. Bashford, and W. M. D. Wright, "Advances in ultrasonic electrostatic transduction," *Ultrasonics*, vol. 36, no. 1, pp. 1–6, Feb. 1998.

[5] A. Gachagan, G. Hayward, S. P. Kelly, and W. Galbraith, "Characterization of air-coupled transducers," *IEEE Trans. Ultrason., Ferroelectr., Freq. Control*, vol. 43, no. 4, pp. 678–689, Jul. 1996.

[6] M. Beck and K. Hinterhofer, "Direct high dynamic flow measurement in the exhaust of combustion engines," *SAE*, vol. SAE 980880, pp. 95–104, 1998.

[7] S. M. Tretiakov, "High precision flow meter for measuring a gaseous volume flow in a pipe," U.S. Patent 6 227 058 B1, May 8, 2001.

[8] ——, "Vorrichtung zur zeitlich hochauflösenden Messung eines gasförmigen Volumenstromes, insbesondere eines Abgas-Volumenstromes eines Verbrennungsmotors, in einem von diesem durchströmten Rohr," Patent Application DE 197 27 960 A1, 1999 (in German).

[9] *Show Daily Monday, World Congress SAE*. (2001, Feb. 4). Warrendale PA: Society of Automotive Engineers. [Online]. Available: http://www.sae.org/congress/2001/showmon.pdf

[10] SickMaihak. (2004). *Datasheet of FLOWSIC 150 CARFLOW*. [Online]. Available: http://www.sickmaihak.de

[11] A. Schröder, S. Harasek, M. Kupnik, M. Wiesinger, E. Gornik, E. Benes, and M. Gröschl, "A capacitance ultrasonic transducer for high temperature applications," *IEEE Trans. Ultrason., Ferroelectr., Freq. Control*, vol. 51, no. 7, pp. 896–907, Jul. 2004.

[12] I. J. O'Sullivan and W. M. D. Wright, "Ultrasonic measurement of gas flow using electrostatic transducers," *Ultrasonics*, vol. 40, no. 1–8, pp. 407–411, May 2002.

[13] A. G. Bashford and D. A. Hutchins, "Air-coupled ultrasonic transducers for measurement of green-state ceramics at elevated temperatures," *Proc. Inst. Elect. Eng.—Sci. Meas. Technol.*, vol. 145, no. 5, pp. 237–243, Sep. 1998.

[14] ——, "Non-destructive evaluation of green-state ceramics using micromachined air-coupled capacitance transducers," *Ultrasonics*, vol. 36, no. 1, pp. 121–126, Feb. 1998.

[15] W. M. D. Wright and D. A. Hutchins, "Monitoring of binder removal from injection molded ceramics using air-coupled ultrasound at high temperature," *IEEE Trans. Ultrason., Ferroelectr., Freq. Control*, vol. 46, no. 3, pp. 647–653, May 1999.

[16] A. Schröder, M. Kupnik, P. O'Leary, E. Benes, and M. Gröschl, "A capacitance ultrasonic transducer for fast flow-measurements in hot pulsating gases," in *Proc. IEEE Sens. Conf.*, 2004, pp. 240–243.

[17] D. W. Schindel, D. A. Hutchins, L. Zou, and M. Sayer, "The design and characterization of micromachined air-coupled capacitance transducer," *IEEE Trans. Ultrason., Ferroelectr., Freq. Control*, vol. 42, no. 1, pp. 42–50, Jan. 1995.

[18] L. C. Lynnworth, Y. Liu, and J. A. Umina, "Extensional bundle waveguide techniques for measuring flow of hot fluids," *IEEE Trans. Ultrason., Ferroelectr., Freq. Control*, vol. 52, no. 4, pp. 538–544, Apr. 2005.

[19] L. C. Lynnworth, *Ultrasonic Measurements for Process Control; Theory, Techniques, Applications*. San Diego, CA: Academic, 1989.

[20] M. Kupnik, A. Schröder, P. O'Leary, E. Benes, and M. Gröschl, "An ultrasonic transit-time gas flowmeter for automotive applications," in *Proc. IEEE Sens. Conf.*, 2004, pp. 451–454.

[21] R. A. Moorman and J. J. Westerkamp, "Maximizing noise-limited detection performance in medium PFR radars by optimizing PFR visibility," in *Proc. IEEE Aerosp. Electron. Conf.*, 1993, pp. 288–293.

[22] P. Brassier, B. Hosten, and F. Vulovic, "High-frequency transducers and correlation method to enhance ultrasonic gas flow metering," *Flow Meas. Instrum.*, vol. 12, no. 3, pp. 201–211, Jun. 2001.

[23] M. Wiesinger, "Entwicklung eines Abgas-Massenflußsensors," Ph.D. dissertation, Vienna Univ. Technol., Vienna, Austria, 1999 (in German).

[24] M. Kupnik, P. O'Leary, A. Schröder, and I. Rungger, "Numerical simulation of ultrasonic transit-time flowmeter performance in high temperature gas flows," in *Proc. IEEE Ultrason. Symp.*, 2003, pp. 1354–1359.

[25] O. Cramer, "The variation of the specific heat ratio and the speed of sound in air with temperature, pressure, humidity, and CO_2 concentration," *J. Acoust. Soc. Amer.*, vol. 93, no. 5, pp. 2510–2516, May 1993.

[26] H. E. Bass, L. C. Sutherland, A. J. Zuckerwar, D. T. Blackstock, and D. M. Hester, "Atmospheric absorption of sound: Further developments," *J. Acoust. Soc. Amer.*, vol. 97, no. 1, pp. 680–683, Jan. 1995.

[27] H. E. Bass, L. C. Sutherland, and A. J. Zuckerwar, "Atmospheric absorption of sound: Update," *J. Acoust. Soc. Amer.*, vol. 88, no. 4, pp. 2019–2021, Oct. 1990.

Mario Kupnik was born in Leoben, Austria, in 1974. He received the M.S. degree in electronics engineering from the Graz University of Technology, Graz, Austria, in 2000 and the Ph.D. degree in physical measurement techniques from the University of Leoben in 2004 for his research in ultrasonic flow metering of hot gaseous mixtures, focusing especially on the exhaust gases of automotive combustion engines.

From summer 1999 to October 2000, he was an Analog Design Engineer with Infineon Technologies AG, Graz, working on the design of ferroelectric memories and contactless smart card systems. From 2000 to 2004, he was a Research Assistant with the Christian Doppler Laboratory for Sensory Measurement, Institute for Automation, University of Leoben. He is currently a Postdoctoral Researcher in the Khuri-Yakub Ultrasonics Group, E. L. Ginzton Laboratory, Stanford University, CA. His research interests include the design and application of capacitive micromachined ultrasonic transducers, focusing especially on ultrasonic transit-time gas flowmeters for hot and pulsating gases, and on ultrasonic nondestructive evaluation. He is the holder of four patents in the fields of analog front-end circuits for contactless smart card systems and ultrasonic transit-time gas flowmeters.

Dr. Kupnik received the 2004 Fred-Margulies Award of the International Federation of Automatic Control (IFAC).

Andreas Schröder was born in Vienna, Austria, in 1972. He received the Ph.D. degree in physics from the Vienna University of Technology (TUW), Vienna, Austria, in 2003.

He was with the Institute of General Physics, TUW, working on the development of capacitance ultrasonic transducers for operation at high temperatures. He continued his work in the field of microelectromechanical systems at the Laboratory for Analysis and Architecture of Systems, National Center for Scientific Research (LAAS-CNRS), Toulouse, France, where his main interest of research was the development of microdeformable mirrors. He is currently with the Acoustic Monitoring Group, Preparatory Commission for the Comprehensive Nuclear-Test-Ban Treaty Organization (CTBTO), Vienna.

Paul O'Leary (M'01) received the B.A. degree in mathematics and the B.A.I. degree in electronics from Trinity College, Dublin, Ireland, in 1982, the M.S. degree in electronic engineering from the PII, Eindhoven, The Netherlands, and the Ph.D. degree from the University of Pavia, Pavia, Italy.

He was with ITT Intermetall, Freiburg im Breisgau, Germany, and headed the Analog and Digital Integrated Circuit Group, AMS Austria Mikro Systeme, Unterpremstätten, Austria. He founded the Institute for Chemical and Optical Sensors, Joanneum Research, Graz, Austria. He received the Chair for Automation at the University of Leoben, Leoben, Austria, in 1995. He directed the Christian Doppler Laboratory for Sensory Measurement from 1996 to 2004 and currently heads the Institute for Automation, University of Leoben. His interests are distributed real-time systems, image processing, and decision support tools.

Ewald Benes (A'97–M'03) was born in Vienna, Austria, in 1943. He received the M.S. and Ph.D. degrees in physics from the Vienna University of Technology (TUW) in 1971 and 1976, respectively. In 1984, he received the habilitation degree at the Faculty of Technology and Natural Science, TUW.

Since 1976, he has been the Leader of the Sensors and Ultrasonics Working Group, Institute of General Physics (IAP), TUW. In 1985, he became an Associate Professor and the Deputy Director of the IAP and has been a Full Professor since 1997. He became the Coordinator of the Ultrasonic Separation of Suspended Particles Network within the Training and Mobility of Researchers Program of the European Commission (http://www.iap.tuwien.ac.at/www/euss), also in 1997. In 2002, he became the Coordinator of the European GROWTH project QxSens (http://www.qxsens.net). In 2004, he was appointed as the Dean of Academic Affairs of the Faculty of Physics, TUW. His present scientific activities are new sensor principles, especially piezoelectric resonators as sensing probes for physical quantities, separation of suspended particles from liquids by ultrasonic resonance fields, and analysis of layered piezoelectric resonator structures. He is a coauthor of more than 110 papers. He is also the holder of 12 patents.

Dr. Benes is a member of the Austrian Physical Society and of the IEEE UFFC Society. Since 1993, he has been a Member of the Steering Committee of the World Congress on Ultrasonics (WCU). In 1996, he was elected as the Founder President of the Austrian Acoustics Association. Since 2000, he has been an Associate Editor of the IEEE SENSORS JOURNAL. He received the Austrian State Award for Energy Research for the development of the energy flow measurement system HELIO-DATA in 1977, which became a national standard for the analysis of multivalent heating systems.

Martin Gröschl was born in Vienna, Austria, in 1959. He received the M.S. and Ph.D. degrees in physics from the Vienna University of Technology (TUW) in 1986 and 1989, respectively. His thesis was dedicated to the development of a novel sensor for beam position control in electron beam evaporation and melting plants. He received the habilitation degree in 1997.

Since 1985, he has been a member of the Sensors and Ultrasonics Working Group, Institute of General Physics, TUW. In 1997, he was promoted to Associate Professor. His main areas of research are the investigation of piezoelectric resonators as sensing probes for physical quantities and the separation of dispersed particles from liquids by means of ultrasonic resonance fields. He is especially engaged in the development of electronic equipment for ultrasonic transducers and measurement systems. Recent work is dedicated to the investigation of capacitance transducers and the development of sensors based on piezoelectric bulk-acoustic-wave resonators. He is the author or coauthor of more than 100 publications, over 50 of which are in refereed journals. He is also the holder of five patents in the fields of electronic instrumentation and ultrasonic separation technology.